Kinematic Design and Commutation of a Spherical Stepper Motor

Gregory S. Chirikjian, *Member, IEEE,* and David Stein, *Student Member, IEEE*

***Abstract*—This paper addresses the design and commutation of a novel kind of spherical stepper motor in which the poles of the stator are electromagnets and the poles of the rotor (rotating ball) are permanent magnets. Due to the fact that points on a sphere can only be arranged with equal spacing in a limited number of cases (corresponding to the Platonic solids), design of spherical stepper motors with fine rotational increments is fundamentally geometrical in nature. We address this problem and the related problem of how rotor and stator poles should be arranged in order to interact to cause motion. The resulting design has a much wider range of unhindered motion than other spherical stepper motor designs in the literature. We also address the problem of commutation, i.e., we determine the sequence of stator polarities in time that approximate a desired spherical motion.**

***Index Terms*—Circle packing, rotation group, spherical motor.**

I. Introduction

THIS paper addresses the design and coordination of spherical motors with a large range of motion. Applications of spherical motors are numerous. They include the following: 1) camera actuators for computer vision [1], as in Fig. 1(a); 2) robotic wrist, elbow, and shoulder actuators, as in Fig. 1(b) (allowing six or nine degrees of freedom to be designed compactly into a small space); 3) omnidirectional wheels for mobile robots, as in Fig. 1(c); and 4) actuator arrays capable of transporting objects in any direction [2], [3], as in Fig. 1(d).

Of course, the concept of a spherical motor is not new. Our work builds on the accomplishments of a number of notable works. The basic operating principles of spherical dc induction motors have been known for quite some time, see, e.g., [4] and [5]. Kaneko *et al.* [6] developed a spherical dc servo motor. The design and implementation of spherical variable-reluctance motors has been studied by Lee *et al.* for a number of years [7]–[10]. Toyama *et al.* have developed spherical ultrasonic motors [11], [12]. In the literature, one even finds actuators with a full six degrees of freedom, e.g., [13]. A good introduction to the principles behind traditional permanent-magnet motors can be found in [14]. These principles are very much the same for the spherical case, although the geometrical aspects in the design are quite different.

In the following sections, we address kinematic issues in the design and commutation of a new spherical stepper motor. In our design, the rotor poles are permanent magnets, and the stator poles are electromagnets. The key issues addressed here are how to arrange the stator and rotor poles so as to achieve relatively finely discretized motion. In contrast to the other spherical motor designs referenced above, we seek to place more poles than the numbers dictated by the regular (Platonic) solids. To this end, Section II examines how rotor and stator poles can be placed "semiregularly" in a recursive fashion with a high degree of symmetry. Section III then examines how to commutate any of a variety of possible motor designs generated using the techniques of Section II. Section IV discusses the design and implementation of a particular stepper motor and provides a detailed example of a commutation sequence.

Manuscript received January 8, 1999; revised August 9, 1999. Recommended by Guest Editor B. Ravani. This work was supported by the National Science Foundation under Grant IIS-9731720 from the Robotics and Human Augmentation Program.

The authors are with the Department of Mechanical Engineering, The Johns Hopkins University, Baltimore, MD 21218 USA.

Publisher Item Identifier S 1083-4435(99)09955-X.

II. The Kinematic Design Problem: Rotor and Stator Pole Placement

Central to the design of spherical motors is the selection of compatible rotor and stator geometries. In the same way that standard cylindrical motors must not have the same number of rotor and stator poles in order to operate, the symmetries of spherical rotors and stators must not be the same. The question then becomes one of finding which combination of stator and rotor arrangements is the most appropriate. Since there is a very limited number of regular arrangements of points on the sphere (there are only five corresponding to the Platonic solids), and since these are far too coarsely distributed for use in a discrete-state motor capable of the applications discussed earlier, the question becomes one of finding compatible "semiregular" rotor and stator arrangements.

It has been known for thousands of years that only five convex three-dimensional polyhedra exist which have polygonal faces that are both congruent and regular. These so-called perfect solids are the tetrahedron (4 triangular faces), cube (6 square faces), octahedron (8 triangular faces), dodecahedron (12 pentagonal faces), and icosahedron (20 triangular faces). By projecting faces of any of these polyhedra onto a sphere from the common center of the sphere and polyhedron, the sphere is divided into regions of equal area and shape. Regular circle packings on the sphere are generated by inscribing circles in each of these regions (which is the same as first inscribing circles in each polygonal face of a perfect solid and then projecting onto the sphere).

The focus of this section is the generation of "semiregular" circle packings on the sphere. These are generated by observing the duality of the perfect solids (i.e., connecting the centers of all adjacent faces of any perfect solid results in another

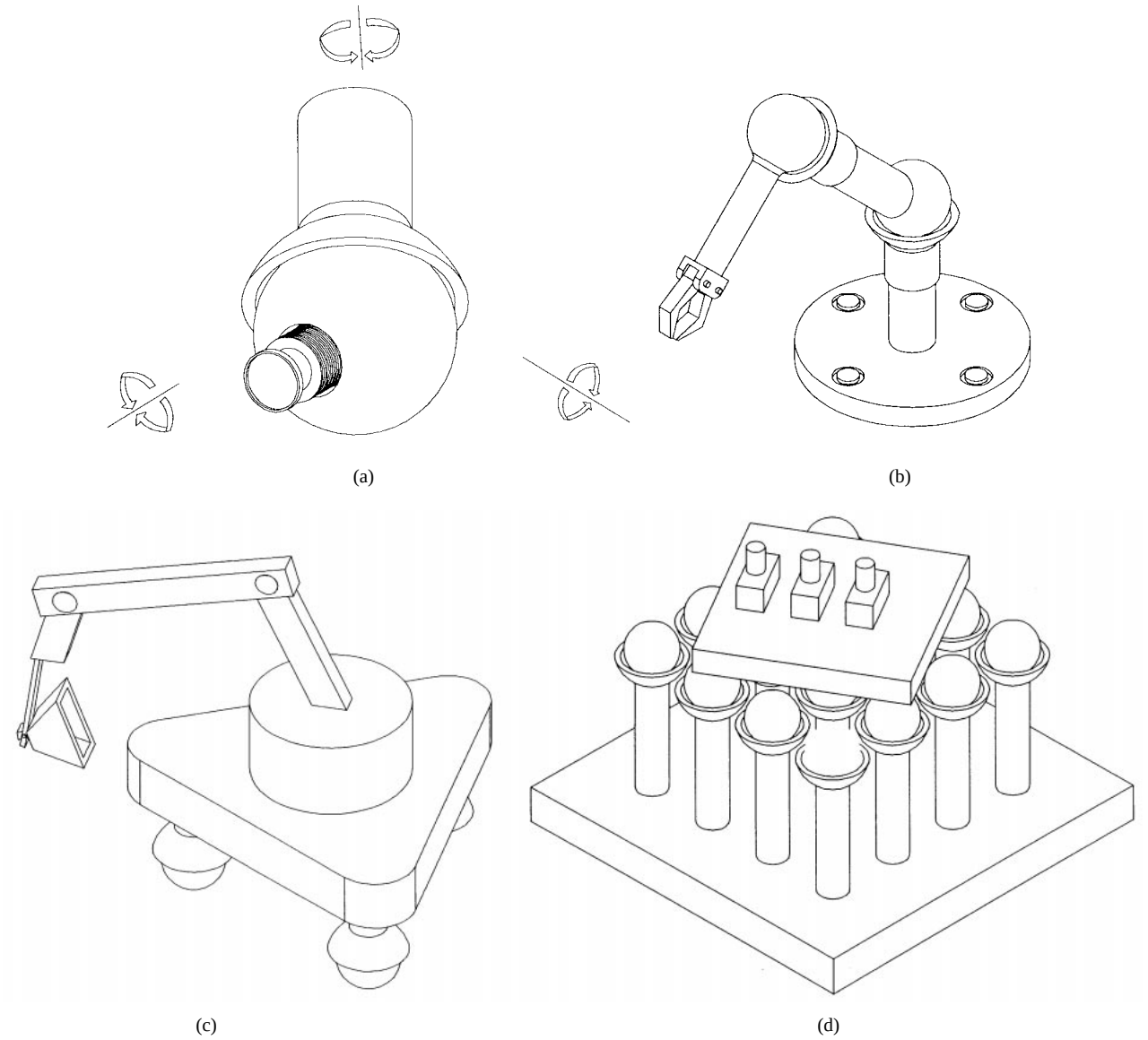

(a) (b) (c) (d)

Fig. 1. Applications of spherical motors.

perfect solid). In particular, the tetrahedron is dual to itself, the cube is dual to the octahedron, the dodecahedron is dual to the icosahedron. A finite group of rotational symmetries exists for each pair of dual perfect solids. By subdividing the sphere into units formed by overlaying the projections of dual perfect solids on the sphere, and observing the symmetries of these units, it is shown below how 16 packings of congruent circles on the sphere are generated in addition to the regular packings. It is then shown how one can pack an arbitrary number of "almost congruent" circles on the sphere by recursively subdividing these units and inscribing circles in each resulting subdivision. In either case, these semiregular packings of congruent circles inherit the symmetry group of their dual parent polyhedra.

Of the 21 regular and semiregular circle packings, two are redundant. The remaining 19 circle packings possess three desirable properties: 1) all circles "kiss" their nearest neighbors; 2) uncovered areas of the sphere surrounded by congruent circles posses discrete rotational symmetry; and 3) uncovered areas surrounded by circles of different size are always enclosed by exactly three circles. These properties form the starting point for a recursion that allows one to pack an arbitrarily large number of incongruent circles on the sphere, the centers of each circle corresponding to the center of a rotor pole. These packings allow one to achieve very high packing ratios, and retain the tetrahedral, cubo–octahedral, or icosa–dodecahedral rotational symmetries of the base semiregular packings of congruent circles.

A. Mathematical Preliminaries

Positions on the unit sphere S^2 are parametrized using spherical coordinates

$$\overline{u}(\phi,\theta) = \begin{pmatrix} \cos\ \phi\ \sin\ \theta \\ \sin\ \phi\ \sin\ \theta \\ \cos\ \theta \end{pmatrix}.$$

θ and ϕ are called the polar and azimuthal angles, respectively.[1]

The distance between two points $\overline{u}_1, \overline{u}_2 \in S^2$ as measured along the shorter segment of the great arc connecting the points is calculated as

$$d(\overline{u}_1, \overline{u}_2) = \cos^{-1}(\overline{u}_1 \cdot \overline{u}_2) \tag{1}$$

where, in the context of the current discussion, $\cos^{-1}(\cdot)$ takes values in the range $[0, \pi]$. In this way, the length of the shorter of the two great arcs connecting $\overline{u}_1$ and $\overline{u}_2$ is automatically chosen.

For example, the distance between the north pole $\overline{c}_3 = [0, 0, 1]^T$ and any arbitrary point $\overline{u}(\phi, \theta)$ is $d(\overline{c}_3, \overline{u}) = \theta$. A *regular* placement of N points on the unit sphere is one for which the distance between each point and its nearest neighbors is the same for all points considered. It has been well known since the time of the ancient Greeks that the only regular placements of points correspond to the vertices of the so-called Platonic solids: tetrahedron, octahedron, cube, icosahedron, and dodecahedron with $N = 4$, 6, 8, 12, and 20, respectively. Fig. 2 shows the icosahedral and octahedral tessellations of the sphere.

As an interesting aside, we note that the simplest spherically shaped viruses encode just enough genetic information to express a single kind of protein unit. A number of these units then self-assemble to form a protein shell. These shells have icosahedral symmetry because this is the regular packing which best approximates a sphere [16], [17]. More sophisticated viruses encode more than one kind of protein which self assemble to form semiregular polyhedral shells. We also note that a number of spherical circle packings in nature can be found in other contexts [18].

Since it is desirable to place rotor and stator poles at finer increments than the vertices of the Platonic solids to achieve finer discretization of rotation, one must consider alternatives to these regular placements.

One approach is to consider the desirable number of stator and rotor poles and pack this number of same-sized circles on the sphere. The centers of these circles then indicate the placement of the centers of the poles. In fact, a wide variety of packings have already been studied in the literature in the context of several different applications (see, e.g., [19]–[21]) An extensive list of spherical circle packings, with up to thousands of circles, is available on the Internet at http://www.research.att.com/~njas.

However, as a rule, such packings do not posses the degree of symmetry that the regular packings do. This is quite important in the context of a spherical stepper, where the rotor and stator poles must have some compatibility in order to be able commutate. Our approach is, therefore, to use *recursive semiregular* packings of almost-equal-sized circles on the sphere. Our search will begin with the vertices of the Platonic solids, and recursively place new points until the desired number is approximated. Then, evaluations of how well disbursed the points are, and how compatible the choice for rotor and stator is, will be performed. In order to do this, we must first develop some mathematical tools to do geometrical constructions on the sphere. Fig. 3 is helpful in this regard.

[1]Often in the engineering literature, the meanings of the symbols θ and ϕ are reversed from our notation (see, e.g., [15]), whereas our notation is consistent with the mathematics and physics literature.

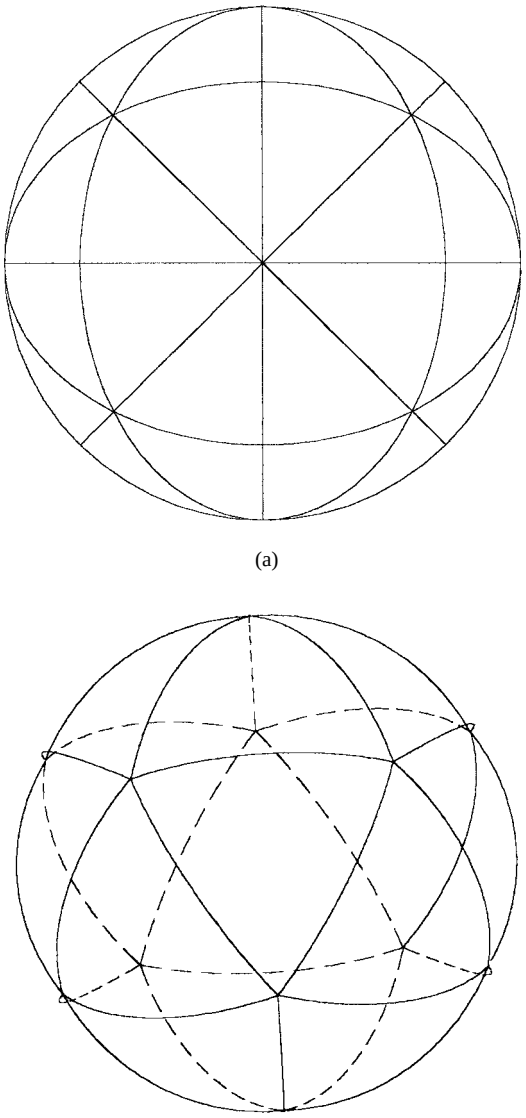

(a)

(b)

Fig. 2. (a) Octahedral and (b) icosahedral discretization of the sphere.

The plane which intersects the sphere resulting in the great circle containing points $\overline{p}$ and $\overline{q}$ has a unit normal

$$\overline{n} = \overline{n}(\overline{p}, \overline{q}) = \frac{\overline{p} \times \overline{q}}{\|\overline{p} \times \overline{q}\|}.$$

The plane containing the great circle which, in turn, contains $\overline{p}$ and $\overline{q}$ is described by

$$\overline{n} \cdot \overline{x} = 0$$

where $\overline{x} \in \mathbb{R}^3$ is the vector of Cartesian coordinates of an arbitrary point.

Given a point on the sphere, $\overline{r}$, one can determine the shortest distance measured on the sphere between $\overline{r}$ and the great circle defined by $\overline{n}$ by first constructing a plane passing through the origin and the point $\overline{r}$ which is orthogonal to the

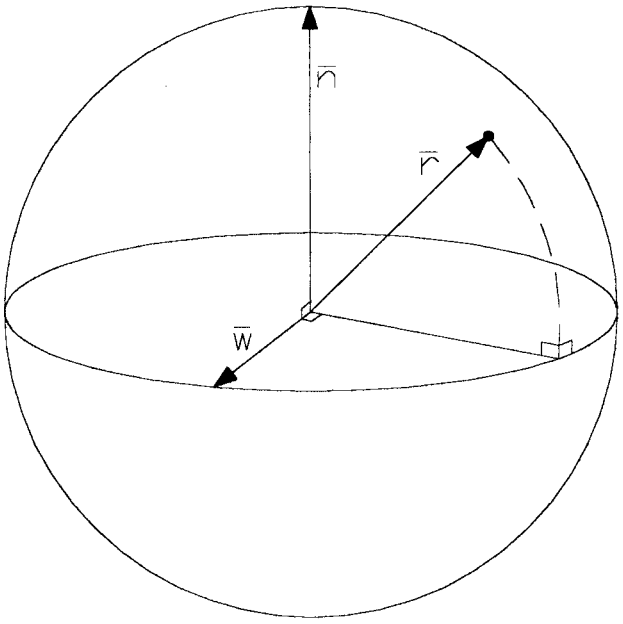

Fig. 3. Distance between a point and great arc.

plane defined by $\overline{n}$. Since $\overline{r}$ and $\overline{n}$ must lie in this new plane, it is defined by the normal

$$\overline{w} = \frac{\overline{r} \times \overline{n}}{||\overline{r} \times \overline{n}||}.$$

The great arc defined by $\overline{w}$ contains $\overline{r}$ and intersects at a right angle the great arc containing $\overline{p}$ and $\overline{q}$. This means the shortest distance between $\overline{r}$ and the great arc defined by $\overline{n}$ is measured along the great arc defined by $\overline{w}$.

The intersection of the two planes, written as the simultaneous equations

$$\overline{n} \cdot \overline{x} = \overline{w} \cdot \overline{x} = 0$$

define a line that intersects the sphere at the points

$$\pm\overline{x} = \pm\frac{\overline{w} \times \overline{n}}{||\overline{w} \times \overline{n}||}.$$

Thus, the distance between $\overline{r}$ and the arc defined by $\overline{n}$ is

$$d_2(\overline{r}, \overline{n}) \triangleq \min\{d(\pm\overline{x}, \overline{r})\}$$

where min simply means minimization with respect to the choice of $\pm$.

Observing that, for $\overline{n}$, $\overline{s} \in S^2$

$$||\overline{r} \times \overline{n}|| = \sqrt{1 - (\overline{r} \cdot \overline{n})^2}$$
$$\overline{n} \times (\overline{r} \times \overline{n}) = \overline{r} - (\overline{n} \cdot \overline{r})\overline{n}$$

and

$$\overline{r} \cdot [\overline{n} \times (\overline{r} \times \overline{n})] = 1 - (\overline{n} \cdot \overline{r})^2$$

one obtains the simple answer

$$d_2(\overline{r}, \overline{n}) = \cos^{-1}[\sqrt{1 - (\overline{r} \cdot \overline{n})^2}].$$

We will use this simple result in the next section to inscribe a spherical cap inside an arbitrary spherical triangle.

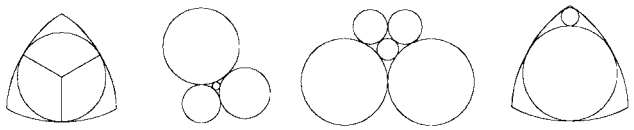

Fig. 4. Inscribing circles within existing geometric structures.

B. Recursive Generation of Circle Packings

To begin, the coordinates of the vertices of the Platonic solids are required. These are calculated as follows, where each solid is centered at the origin, and the vertices all lie on the surface of the unit sphere S^2.

Tetrahedron: The spherical coordinates of the first vertex can be taken as $(\phi, \theta) = (0, 0)$ (the north pole). The remaining three vertices have spherical coordinates $(0, \alpha)$, $(2\pi/3, \alpha)$, and $(4\pi/3, \alpha)$. The polar angle α is determined by the equality

$$d(\overline{u}(0,0), \overline{u}(0,\alpha)) = d(\overline{u}(2\pi/3, \alpha), \overline{u}(0,\alpha)).$$

Octahedron: The vertices lie at $\overline{v}_1 = (0,0,1)^T$, $\overline{v}_2 = (0,0,-1)^T$, $\overline{v}_3 = (1,0,0)^T$, $\overline{v}_4 = (-1,0,0)^T$, $\overline{v}_5 = (0,1,0)^T$, $\overline{v}_6 = (0,-1,0)^T$.

Cube: The vertices lie at $\overline{v}_1 = (1/\sqrt{3})(1,1,1)^T$, $\overline{v}_2 = (1/\sqrt{3})(-1,1,1)^T$, $\overline{v}_3 = (1/\sqrt{3})(1,-1,1)^T$, $\overline{v}_4 = (1/\sqrt{3})(1,1,-1)^T$, $\overline{v}_5 = (1/\sqrt{3})(-1,-1,1)^T$, $\overline{v}_6 = (1/\sqrt{3})(1,-1,-1)^T$, $\overline{v}_7 = (1/\sqrt{3})(-1,1,-1)^T$, $\overline{v}_8 = (1/\sqrt{3})(-1,-1,-1)^T$.

Icosahedron: It is clear from its symmetry that $\overline{v}_1 = (0,0,1)^T$, $\overline{v}_2 = (0,0,-1)^T$. Then, there are two sets of five points with coordinates as follows. The first set has coordinates $(0, \beta)$, $(\pi/5, \beta)$, $(2\pi/5, \beta)$, $(3\pi/5, \beta)$, and $(4\pi/5, \beta)$. The second set is rotated about the $\overline{e}_3$ axis by $\pi/10$ relative to the first, and is as distant from the south pole as the other set is from the north pole: $(\pi/10, \pi - \beta)$, $(3\pi/10, \pi - \beta)$, $(5\pi/10, \pi - \beta)$, $(7\pi/10, \pi - \beta)$, and $(9\pi/10, \pi - \beta)$. The angle β is determined by

$$d(\overline{v}_1, \overline{u}(0,\beta)) = d(\overline{u}(0,\beta), \overline{u}(\pi/10, \pi - \beta))$$

or

$$d(\overline{v}_1, \overline{u}(0,\beta)) = d(\overline{u}(0,\beta), \overline{u}(\pi/5, \beta)).$$

Dodecahedron: The vertices are determined by taking all sets of three most proximal vertices of the icosahedron, adding them, and normalizing so that the result is a unit vector.

1) Inscribing Circles in Triangular Regions on the Sphere: Any three points $\overline{p}$, $\overline{q}$, $\overline{r} \in S^2$ define the vertices of a spherical triangle. Therefore, they define the spherical triangle. In this section, we solve the following: given these points, find a fourth point that is simultaneously equidistant from the three edges of the spherical triangle and, hence, defines the center of an inscribed circular cap (see Fig. 4).

This can be stated as the solution $\overline{x} \in S^2$ of the set of equations

$$d_2(\overline{x}, \overline{n}_1) = d_2(\overline{x}, \overline{n}_2) = d_2(\overline{x}, \overline{n}_3)$$

where $\overline{n}_1 = \overline{n}(\overline{p}, \overline{q})$, $\overline{n}_2 = \overline{n}(\overline{p}, \overline{r})$, and $\overline{n}_3 = \overline{n}(\overline{r}, \overline{q})$.

This problem can be restated as the three equations

$$(\overline{n}_1 - \overline{n}_2) \cdot \overline{x} = 0$$
$$(\overline{n}_3 - \overline{n}_2) \cdot \overline{x} = 0$$
$$\overline{x} \cdot \overline{x} = 1.$$

Clearly, $\overline{x}$ satisfies the first two equations when it is a scalar multiple of the cross product of $\overline{n}_1 - \overline{n}_2$ and $\overline{n}_3 - \overline{n}_2$. The last equation is satisfied by normalizing this result. Hence,

$$\overline{x} = \pm \frac{(\overline{n}_1 - \overline{n}_2) \times (\overline{n}_3 - \overline{n}_2)}{|(\overline{n}_1 - \overline{n}_2) \times (\overline{n}_3 - \overline{n}_2)|}.$$

The two choices correspond to the same circle in $\mathbb{R}^3$, but different circular caps with antipodal centers and radii r and $\pi - r$. That is, for every spherical circular cap, there is another which is its complement in the sphere. We choose the value of $\overline{x}$ for which the radius as measured on the sphere is smaller. Using this general result, one can inscribe circles in the spherical triangles that result from subdividing the spherical polygons generated by connecting the vertices listed in the previous section.

2) Inscribing Spherical Circles in the Space Between Existing Spherical Circles: Suppose one is given three kissing circles on the surface of the sphere, with centers $\overline{p}_1, \overline{p}_2, \overline{p}_3$, and radii r_1, r_2, and r_3 as measured on the surface of the sphere. Then, to find the center of a circle inscribed in the space between the three circles, one solves the system of equations

$$d(\overline{x}, \overline{p}_i) = r + r_i, \qquad \overline{x} \cdot \overline{x} = 1 \tag{2}$$

for $i = 1, 2, 3$ where $\overline{x}$ is the unknown position of the center of the desired circle, and r is its radius. This system of equations is solvable in closed form as follows.

First, take the cosine of (2) for each value of i, and expand the right side using trigonometric rules. The result is written in matrix form as

$$\begin{pmatrix} \overline{p}_1^T \\ \overline{p}_2^T \\ \overline{p}_3^T \end{pmatrix} \overline{x} = \mathbf{A}\overline{r} \tag{3}$$

where

$$\mathbf{A} = \begin{pmatrix} \cos\ r_1 & -\sin\ r_1 \\ \cos\ r_2 & -\sin\ r_2 \\ \cos\ r_3 & -\sin\ r_3 \end{pmatrix}$$

and

$$\overline{r} = \begin{pmatrix} \cos\ r \\ \sin\ r \end{pmatrix}.$$

Hence, once r is known, $\overline{x}$ can be found by a simple matrix inversion. r is found by isolating $\overline{x}$ in (3), and writing the dot product

$$1 = \overline{x} \cdot \overline{x} = \overline{r}^T B \overline{r} = b_{11}\ \cos^2 r + 2b_{12}\ \sin\ r\ \cos\ r + b_{22}\ \sin^2\ r.$$

Making the standard substitutions

$$\cos^2\ r = (\cos\ 2r + 1)/2$$
$$\sin^2\ r = (1 - \cos\ 2r)/2$$
$$2\ \sin\ r\ \cos\ r = \sin\ 2r$$

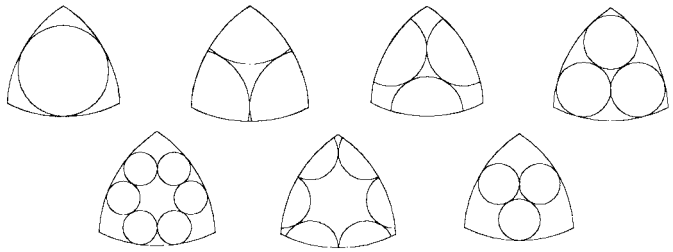

Fig. 5. Enumeration of semiregular circle packings.

and

$$\cos\ 2r = \frac{1 - z^2}{1 + z^2}$$
$$\sin\ 2r = \frac{2z}{1 + z^2}$$

the equation $1 = \overline{r}^T B \overline{r}$ reduces to a quadratic equation in z with two roots for r. The smallest positive real root is then chosen, and backsubstitution yields $\overline{x}$.

The problem of finding the inscribed circle within four touching circles, the problem of inscribing a circle in a spherical quadrilateral with symmetry, and the problem of finding the circle inscribed in the space between a spherical triangle and an already-existing inscribed circle follow similarly.

3) Enumeration of Semiregular Spherical Circle Packings: Once the sphere is tessellated into congruent regular spherical triangles, there are seven ways to inscribe circles within and between these triangles. These are depicted in Fig. 5. Using the techniques outlined previously, and knowing the coordinates of all the vertices, the positions of the centers of these circles (which we refer to as *primary circles*) and their radii are easily calculated.

Doing the enumeration explicitly, one finds that two sets of semiregular circle packings are shared between those with octahedral and tetrahedral symmetry. Hence, the number of distinct semiregular packings is 19 (5 Platonic + 14 others).

These semiregular packings form the starting point for a recursive procedure in which circles can be inscribed within collections of kissing circles to fill the remaining empty spaces. Particularly promising semiregular packings are: 1) the one with icosahedral symmetry with six half circles per triangle, and two other sized circles inscribed in the center and at the vertices and 2) the one with octahedral symmetry and six primary circles inscribed per triangle, with smaller ones inscribed around them. In this way, the primary circles from both packings are almost the same size and, since the symmetry groups of the packings are not the same, there will never be a state from which the motor is unable to escape. It would seem that choosing any two of the 19 distinct packings from different symmetry categories is a prerequisite for rotor and stator compatibility. It is also important that a sufficient number of rotor and stator poles line up to generate narrow potential wells corresponding to stepper states. Our choice satisfies this requirement as well.

III. Mathematical Formulations of the Commutation Problem

In this section, the commutation problem is addressed.

In the two subsequent sections, the problem is addressed using two different perspectives. In Section III-A, a purely geometrical approach based on spherical distances between the centers of rotor and stator poles is examined. In Section III-B, a functional-analytic approach in which a simplified model of the interference between rotor and stator magnetic fields is used to determine the best matching to implement a desired motion.

A. Geometric Approach

We discretize any given rotational trajectory $R(t)$ into n segments corresponding to $n+1$ points $t_0, \cdots, t_n$. The values t_i can be taken as the even discretization of time $t_i = i/n$, or as the solution generated from a motion interpolation procedure imposing the requirement that the "rotational distance" between adjacent rotations be equal for some measure of distance between rotations

$$D(R_{i-1}, R_i) = D(R_i, R_{i+1}).$$

Such interpolation procedures are described in [23]–[25] and [27] for a variety of different distance (metric) functions.

The distance function for rotations introduced to the mechanical design community by Park [24] is particularly physically meaningful and easy to calculate, as explained below.

A general rotation is written as

$$\begin{aligned} R &= \mathrm{ROT}[\overline{n}, \theta] = \exp[\theta N] \\ &= 1_{3\times 3} + (\sin\ \theta)N + (1 - \cos\ \theta)N^2 = Q_i \mathrm{ROT}[\overline{e}_i, \theta] Q_i^T \end{aligned}$$

where N is the skew symmetric matrix satisfying $N\overline{x} = \overline{n} \times \overline{x}$ for all $\overline{x} \in \mathbb{R}^3$, $\overline{n} \triangleq \mathrm{vect}(N)$ is the unit vector specifying the axis of rotation, and θ is the angle of rotation. $1_{3\times 3}$ is the 3×3 identity matrix. The rotations about the natural basis vectors $\overline{e}_i$ are denoted $\mathrm{ROT}[\overline{e}_i, \theta]$, and Q_i is any rotation matrix whose ith column is the vector $\overline{n}$. The functions [26]

$$\theta(R) = \cos^{-1}\left(\frac{tr(R) - 1}{2}\right)$$

and

$$\overline{n}(R) = \frac{1}{2\sin\theta(R)} \mathrm{vect}(R - R^T)$$

can be thought of as those which extract the angle θ and axis $\overline{n}$ from the rotation matrix $R = \mathrm{ROT}[\overline{n}, \theta]$. Park's metric is then

$$D(R_1, R_2) = \theta(R_1^T R_2) = \theta(R_2^T R_1).$$

Regardless of how the values $\{t_i\}$ and, hence, the matrices $R_i = R(t_i)$, are generated, the problem reduces at each value of i to find an optimal match between at least two stator and rotor poles that are attainable given the current actual orientation $\tilde{R}_i$.[2]

[2] Fixing only two points on the surface of the sphere (which do not lie on the same axis through its center) is required to fix the orientation of the sphere whose origin is already fixed.

Since the motor has discrete states, in general, $\tilde{R}_i \neq R_i$, but $D(\tilde{R}_i, R_i)$ is minimal under the constraints of the motor design and motion history dictated by the desired trajectory.

Given the set of N stator poles $\{\overline{v}_k\}$ and the set of M rotor poles $\{\overline{u}_j\}$, one can sort the distances $d_{jk}(i) = \cos^{-1}((R_i\overline{u}_j) \cdot \overline{v}_k)$ for each desired rotation R_i to find candidates for the matching that would best implement the desired rotation. In general, none of these matchings will yield the desired rotation R_i, but rather a set of approximations $\{\tilde{R}_i^{(m)}\}$ for $m = 1, \cdots, N_1 < N$. The one matching that is chosen from this set is then denoted as $\tilde{R}_i$. In order to arrive at this choice, the list of candidates is reduced based on two criteria.

- All candidates for which the $SO(3)$ distance $D(\tilde{R}_i^{(m)}, \tilde{R}_{i-1})$ are too large to achieve for the given motor design are excluded.
- Even if the transition from $\tilde{R}_{i-1}$ to $\tilde{R}_i$ is within the reach of a single step, it is desirable to have the axis of the relative rotation $\tilde{R}_{i-1}^T \tilde{R}_i^{(m)}$ point as much as possible along the direction of the axis of $\tilde{R}_{i-1}^T R_i$. Hence, the remaining candidates are reduced to a single candidate by finding the one which minimizes the cost function

$$c(\tilde{R}_{i-1}, R_i, \tilde{R}_i^{(m)}) = \cos^{-1}(\overline{n}(\tilde{R}_{i-1}^T \tilde{R}_i^{(m)}) \cdot \overline{n}(\tilde{R}_{i-1}^T R_i)).$$

If the motor is properly designed, at each step there will be a nonempty set of possible moves. If more than one choice exists, it is possible for the sequence $\{\tilde{R}_i\}$ for $i = 0, \cdots, n$ to not be uniquely specified by the sequence of desired rotations $\{R_i\}$.

The drawback of this approach is that it is a purely kinematical model, and does not take into account the electromechanics of the stator–rotor interaction. For instance, if two stator coils are activated and they do not exactly line up with the rotor poles, then an equilibrium orientation will be established which is governed by the minimum of a potential energy function. In the next section, we present an approach which approximates the effects of magnetic field strength with a purely phenomenological potential energy function.

B. Planning Using Potential Functions

The approach to the commutation problem presented in the previous section does not explicitly account for the spatial variability of the magnetic field strength of the electromagnets in the stator assembly and permanent magnets in the rotor poles. Here, we do not explicitly solve the electromagnetics from Maxwell's laws. This is an involved problem requiring simplifying assumptions, as pointed out in [10]. One such assumption in the context of the design in [10] is that the reluctance force (the force which aligns rotor and stator poles) is proportional to the area of overlap between the poles. Within this model, the area on the sphere corresponding to the kth stator can be thought of as a window function, $w(\overline{u}(\theta, \phi), \overline{v}_k, r_s)$ on the sphere which is constant on the spherical circle of radius r_s centered at $\overline{v}_k$ and zero otherwise. Likewise, the function $w(\overline{u}(\theta, \phi), R\overline{u}_i, r_r)$ corresponds to the ith rotor pole of radius r. Then, the overlapping area can be calculated as the integral over the sphere of the absolute value of the difference of these functions, or equivalently in the

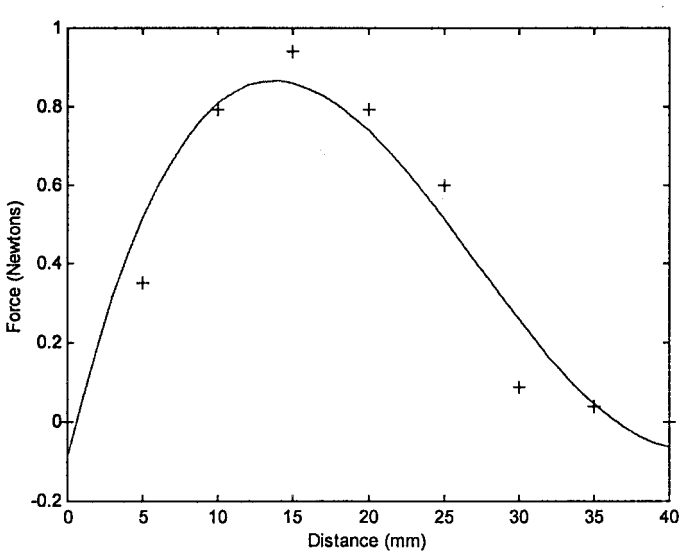

(a)

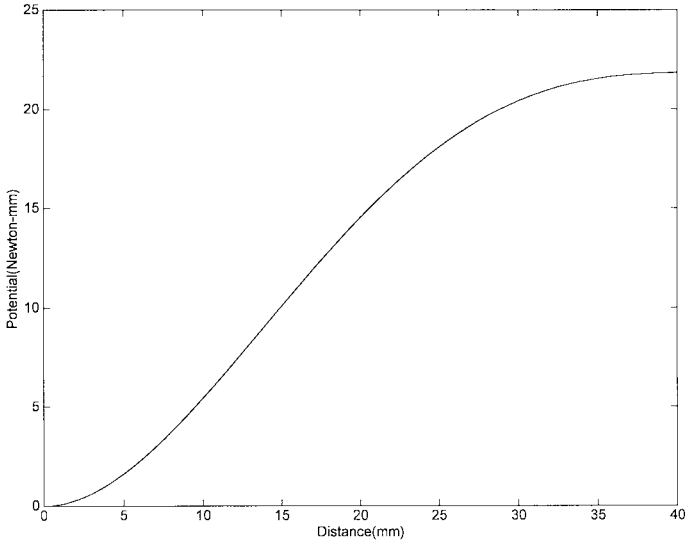

(b)

Fig. 6. (a) Actual and model force relation and (b) potential function.

context of this example, the square root of the integral of the square of the difference of these functions.

More generally, we approximate the interaction of the magnetic fields of one rotor pole and one stator pole as a potential function

$$V(R) = \int_{\theta=0}^{\pi} \int_{\phi=0}^{2\pi} |f_1(\overline{u}(\theta,\phi), R\overline{u}_i) - f_2(\overline{u}(\theta,\phi), \overline{v}_i)|^2 \cdot \sin\ \theta\ d\theta\ d\phi. \quad (4)$$

The potential for multiple poles follows in a similar way. The functions f_i need not be piecewise constant. Based on force measurements of the interaction between electromagnets used in the stators and permanent magnets used in the rotor, one can choose an "ansatz" for f_i and fit parameters so that $V(R)$ matches the data. We note that this model is purely phenomenological and was chosen because it has the correct qualitative performance.

Fig. 6 graphs the actual measured force, and an analytical approximation of force with the best fourth-order polynomial fit. The approximate potential function is then found analytically from the force–displacement curve. The experiment was performed by translating a rotor magnet in the plane whose normal is the axis of the stator, since this is a convenient measurement to take. Small rotations of the rotor are approximated well as translations [27], and so we use this translational data as the starting point for fitting our ansatz.

In the subsequent two sections, we present the mathematics required to approximate these functions on the sphere using spherical harmonics, and write the rotated versions of these functions in an analytically tractable way. In Section III-B-3, we show how these techniques are applied to the problem at hand.

1) Orthonormal Expansions on the Sphere: The spherical harmonics that are used to expand functions on the sphere are given as [32][3]

$$Y_l^m(\theta,\phi) = \sqrt{\frac{(2l+1)(l-m)!}{4\pi(l+m)!}}\ P_l^m(\cos\ \theta) e^{im\phi}. \quad (5)$$

These are called harmonics, because they are eigenfunctions of the Laplacian operator, i.e., they are solutions to the equation

$$\nabla^2 u = \lambda u$$

where $\lambda = -l(l+1)$ and the Laplacian for the sphere is defined as [15]

$$\nabla^2 = \frac{1}{\sin\ \theta}\ \frac{\partial}{\partial\theta}\left(\sin\ \theta \frac{\partial}{\partial\theta}\right) + \frac{1}{\sin^2\ \theta}\ \frac{\partial^2}{\partial\phi^2}.$$

As a general rule, the eigenfunctions of the Laplacian on any compact-oriented Riemannian manifold, M, forms a complete orthonormal series with which to approximate any member of the set of square-integrable functions on the manifold, $\mathcal{L}^2(M)$. Hence, as a special case, any function in $\mathcal{L}^2(S^2)$ can be expanded in a *(spherical) Fourier series* as

$$f(\theta,\phi) = \sum_{l=1}^{\infty} \sum_{m=-l}^{l} \hat{f}(l,m) Y_l^m(\theta,\phi) \quad \text{where}$$

$$\hat{f}(l,m) = \int_{S^2} f\overline{Y_l^m}\ ds. \quad (6)$$

Here, we use the notation

$$\int_{S^2} f\ ds = \int_{\theta=0}^{\pi} \int_{\phi=0}^{2\pi} f(\theta,\phi)\ \sin\ \theta\ d\theta\ d\phi.$$

The collection of coefficients $\hat{f}(l,m)$ is called the *(spherical) Fourier transform* (or spectrum) of $f(\theta,\phi)$. The Plancherel (Parseval) equality holds as

$$\int_{S^2} |f|^2\ ds = \sum_{l=1}^{\infty} \sum_{m=-l}^{l} |\hat{f}(l,m)|^2.$$

Both the Plancherel and reconstruction formulas follow easily from the orthonormality of the spherical harmonics

$$\int_{S^2} Y_l^m \overline{Y_{l'}^{m'}}\ ds = \delta_{ll'}\delta_{mm'}$$

and their completeness.

[3]Note that spherical harmonics are often defined as $\bar{Y}_l^m = (-1)^m Y_l^m$.

It is interesting to note that, while the Abelian fast Fourier transform (FFT), which dates back to the time of Gauss, and was rediscovered by Cooley and Tukey [28], is quite old and well known, an FFT and inversion formula for the sphere developed by Driscoll and Healy is quite modern [29].

2) Orthogonal Expansions on the Rotation Group: Functions on the rotation group $SO(3)$ can be expanded in harmonics in a similar way to functions on the sphere. When ZXZ Euler angles are used

$$R(\alpha,\beta,\gamma) = R_3(\alpha)R_1(\beta)R_3(\gamma)$$

where $R_i(\theta) = \mathrm{ROT}[\overline{e}_i,\theta]$. In this parameterization, the Laplacian on $SO(3)$ is given as

$$\nabla^2 = \frac{\partial^2}{\partial\beta^2} + \cot\beta\,\frac{\partial}{\partial\beta} + \frac{1}{\sin^2\beta}\cdot\left(\frac{\partial^2}{\partial\alpha^2} - 2\cos\beta\,\frac{\partial^2}{\partial\alpha\partial\gamma} + \frac{\partial^2}{\partial\gamma^2}\right). \quad (7)$$

The eigenfunctions $u(\alpha,\beta,\gamma)$ which satisfy

$$\nabla^2 u = \lambda u$$

can be found using separation of variables.[4] They are written as $U^l_{mn}(R(\alpha,\beta,\gamma))$ for $l = 0,1,2,\cdots$ and $|m|,|n| \le l$, and again solve the problem for $\lambda = -l(l+1)$. These harmonics can be viewed as the matrix elements of the $(2l+1)\times(2l+1)$ dimensional matrices U^l, called the irreducible unitary representations of $SO(3)$ [31]–[33]. These matrix elements are given by

$$U^l_{mn}(R(\alpha,\beta,\gamma)) = i^{m-n}e^{-i(m\alpha+n\gamma)}P^l_{mn}(\cos\beta). \quad (8)$$

In the literature, a range of equivalent formulas for these eigenfunctions are provided. For instance, it is often convenient to consider the representations of $SO(3)$ parametrized in ways other than ZXZ Euler angles. When ZYZ Euler angles are used

$$\begin{aligned} &R_3(\alpha)R_2(\beta)R_3(\gamma)\\ &\quad = R_3(\alpha)(R_3(\pi/2)R_1(\beta)R_3(-\pi/2))R_3(\gamma)\\ &\quad = R_3(\alpha+\pi/2)R_1(\beta)R_3(\gamma-\pi/2) \end{aligned}$$

and so

$$R_{ZYZ}(\alpha,\beta,\gamma) = R_{ZXZ}(\alpha+\pi/2,\beta,\gamma-\pi/2).$$

Hence, when one evaluates the matrix elements (8), one finds

$$\begin{aligned} U^l_{mn}(R_{ZYZ}(\alpha,\beta,\gamma)) &= e^{+i(n-m)\pi/2}U^l_{mn}(R_{ZXZ}(\alpha,\beta,\gamma))\\ &= e^{-im\alpha}P^l_{mn}(\cos\beta)e^{-in\gamma} \end{aligned} \quad (9)$$

since the factor $e^{+i(n-m)\pi/2} = i^{n-m}$ cancels with the i^{m-n} in (8). The matrix elements in (9) are often referred to in the physics literature as the *Wigner D-functions* [32].

The functions $P^l_{mn}(\cos\beta)$ are generalizations of the associated Legendre functions, and are given by the Rodrigues formula [32]

$$\begin{aligned} P^l_{mn}(x) = \frac{(-1)^{l-m}}{2^l}&\left[\frac{(l+m)!}{(l-n)!(l+n)!(l-m)!}\right]^{1/2}\\ &\cdot(1+x)^{-(m+n)/2}\times(1-x)^{(n-m)/2}\\ &\cdot\frac{d^{l-m}}{dx^{l-m}}\left[(1-x)^{l-n}(1+x)^{l+n}\right]. \end{aligned} \quad (10)$$

These functions satisfy certain symmetry relations, including

$$\begin{aligned} P^l_{mn}(x) &= (-1)^{m+n}P^l_{nm}(x)\\ P^l_{mn}(x) &= (-1)^{m-n}P^l_{-m,-n}(x) \quad (11)\\ P^l_{mn}(x) &= P^l_{-n,-m}(x)\\ P^l_{mn}(x) &= (-1)^{l+n}P^l_{-m,n}(-x). \quad (12) \end{aligned}$$

They also satisfy certain recurrence relations, including those shown at the bottom of the page [31]–[33],[5] where $c^l_n = \sqrt{(l+n)(l-n+1)}$. Note that $c^l_{-n} = c^l_{n+1}$. The above recurrence relations are key in the efficient calculation of the FFT on the rotation group [30].

Furthermore, they can be related to functions of classical physics such as the Legendre polynomials

$$P_l(x) = P^l_{00}(x)$$

and the associate Legendre polynomials

$$P^n_l(x) = C_n\left[\frac{(l+n)!}{(l-n)!}\right]^{1/2}P^l_{-n,0}(x)$$

where $C_n = 1$ for $n>0$ and $C_n = (-1)^n$ for $n<0$.

It is easy to see that given the orthogonality and completeness properties of the functions U^l_{mn} (which follow because they are eigenfunctions of the Laplacian) that

$$\int_{SO(3)} U^l_{mn}(R)U^s_{pq}(R)\,d\mu(R) = \frac{1}{2l+1}\,\delta_{ls}\delta_{mp}\delta_{nq}.$$

[4]Note that the Laplacian for $SO(3)$ degenerates to that on S^2 if u has no dependence on α (or γ).

[5]Our notation is consistent with Vilenkin and Klimyk [32]. The functions that Gel'fand *et al.* [31] call P^l_{mn} differ from ours by a factor of i^{m-n}, which results in slightly different looking recurrence relations. Varshalovich *et al.* use ZYZ Euler angles. Their relations are different from ours by a factor of $(-1)^{m-n}$.

$$\cos\beta P^l_{mn} = \frac{[(l^2-m^2)(l^2-n^2)]^{1/2}}{l(2l+1)}P^{l-1}_{mn} + \frac{mn}{l(l+1)}P^l_{mn} + \frac{[(l+1)^2-m^2]^{1/2}[(l+1)^2-n^2]^{1/2}}{(l+1)(2l+1)}P^{l+1}_{mn}$$

$$\frac{1}{2}c^l_{-n}P^l_{m,n+1} + \frac{1}{2}c^l_nP^l_{m,n-1} = \frac{m-n\cos\beta}{\sin\beta}P^l_{mn}$$

$$-\frac{1}{2}c^l_mP^l_{m-1,n} - \frac{1}{2}c^l_{-m}P^l_{m+1,n} = \frac{n-m\cos\beta}{\sin\beta}P^l_{mn}$$

In ZXZ Euler angles

$$\int_{SO(3)} f(R)\, d\mu(R) = \frac{1}{8\pi^2} \int_{\beta=0}^{\pi} \int_{\alpha=0}^{2\pi} \int_{\gamma=0}^{2\pi} f(\alpha,\beta,\gamma) \cdot \sin\ \beta\, d\beta\, d\alpha\, d\gamma.$$

The factor $1/8\pi^2$ is the normalization such that $\int_{SO(3)} d\mu(R) = 1$. Hence, we expand functions in $\mathcal{L}^2(SO(3))$ in a Fourier series as

$$f(R) = \sum_{l=0}^{\infty} (2l+1) \sum_{m=-l}^{l} \sum_{n=-l}^{l} \hat{f}^l_{nm} U^l_{mn}(R) = \sum_{l=0}^{\infty} (2l+1)\, \mathrm{trace}[\hat{f}^l U^l] \tag{13}$$

where

$$\hat{f}^l_{mn} = \int_{SO(3)} f(R) U^l_{mn}(R^{-1})\, d\mu(R). \tag{14}$$

We state without proof that the homomorphism property $U^l(R_1 \circ R_2) = U^l(R_1)U^l(R_2)$ holds, and that $\{U^l\}$ for $l = 0, 1, 2, \cdots$ is a complete set of irreducible unitary representations for $SO(3)$. Taking these facts for granted, the Plancherel equality

$$\int_{SO(3)} |f(R)|^2\, d\mu(R) = \sum_{l=0}^{\infty} (2l+1)\, \|\hat{f}^l\|_2^2$$

and convolution theorem

$$(f_1 * f_2)\hat{} = \hat{f}^l_2 \hat{f}^l_1$$

hold as special cases of the general theory, where $\|\cdot\|_2$ is the Hilbert–Schmidt norm, and convolution is defined in the group theoretical context as

$$(f_1 * f_2)(R) = \int_{SO(3)} f_1(Q) f_2(Q^{-1}R)\, d\mu(Q).$$

See [33] and [34] for details.

When ZYZ Euler angles are used, the $SO(3)$ matrix elements U^l_{mn} are related to the spherical harmonics as

$$U^l_{m0}(R_{ZYZ}(\alpha,\beta,\gamma)) = e^{-im\alpha} P^l_{m0}(\cos\ \beta) = (-1)^m \sqrt{\frac{4\pi}{2l+1}}\, \overline{Y^m_l}(\beta,\alpha)$$

and

$$U^l_{0n}(R_{ZYZ}(\alpha,\beta,\gamma)) = P^l_{0n}(\cos\ \beta) e^{-in\gamma} = \sqrt{\frac{4\pi}{2l+1}}\, \overline{Y^n_l}(\beta,\gamma).$$

It follows from the homomorphism property that

$$U^l_{0n}(R_1 R_2) = \sum_{m=-l}^{l} U^l_{0m}(R_1) U^l_{mn}(R_2).$$

This means

$$\overline{Y^n_l}(\theta',\phi') = \sum_{m=-l}^{l} \overline{Y^m_l}(\theta,\phi) U^l_{mn}(\alpha,\beta,\gamma) \tag{15}$$

where θ' and ϕ' are the transformed spherical coordinates such that

$$\overline{u}' = \overline{u}(\theta',\phi') = R_{ZYZ}(\alpha,\beta,\gamma)\overline{u}(\theta,\phi) = R\overline{u}.$$

Using the notation $Y^m_l(\overline{u}(\theta,\phi)) = Y^m_l(\theta,\phi)$ and conjugating both sides of (15), one writes

$$Y^n_l(R\overline{u}) = \sum_{m=-l}^{l} \overline{U^l_{mn}(R)} Y^m_l(\overline{u}).$$

Substitution of R^T for R and using the unitarity of the representations U^l gives

$$Y^n_l(R^T\overline{u}) = \sum_{m=-l}^{l} U^l_{nm}(R)\, Y^m_l(\overline{u}). \tag{16}$$

In summary, the $SO(3)$ harmonics provide a tool to express the rotated version of a function on the sphere expanded in terms of spherical harmonics. The $SO(3)$ harmonics also are used to expand functions on $SO(3)$ and, when such functions are constant on isotropy subgroups isomorphic to $SO(2)$, they reduce down to functions on $SO(3)/SO(2) \cong S^2$ which are scalar multiples of the spherical harmonics.

3) Applications to Our Model: A stator pole can be taken as the north pole. As the rotor rotates, the potential becomes a function of rotation. For a scalar-valued function of $S^2 \times S^2$-valued argument like $f_1(\overline{u}, R\overline{v})$ in (4), one has

$$f(\overline{u}, R\overline{v}) = f(R^T\overline{u}, \overline{v}).$$

Hence, approximating f_1 and f_2 in the ansatz potential (4) using spherical harmonics and using (16) allows for a neat way of writing the potential $V(R)$. Without using this technique to simplify the form of the integrands in the potential function, the integration in (4) would have to be evaluated for each R. With the tools of Section III-B-2, the integration can be performed independent of R.

IV. Implementation of the Prototype

The implementation of our spherical stepper motor was achieved by placing cylindrical rare-earth permanent magnets along the inside surface of a hollow plastic sphere (with magnetic poles aligned with axes of the sphere) to form the rotor.

The stator consists of off-the-shelf wrapped soft iron cores placed on the outside of a spherical cap which are polarized to form electromagnetic fields. Due to the fact that the symmetry of the rotor pole arrangement is different than that of the stator poles, the fields created by energizing stator coils provide a torque that changes the orientation of the rotor.

A key feature of our design that is different than others found in the literature is that the stator does not envelop the rotor. In fact, it covers less than a hemisphere. As a result, our design is able to achieve a very wide range of motion.

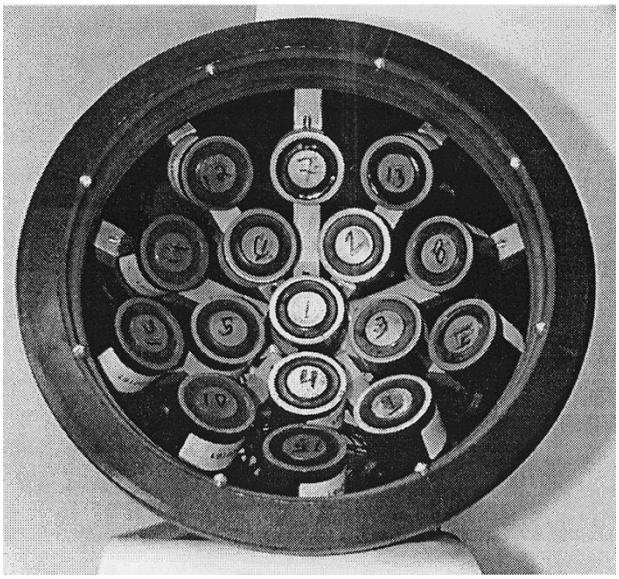

Fig. 7. Stator assembly.

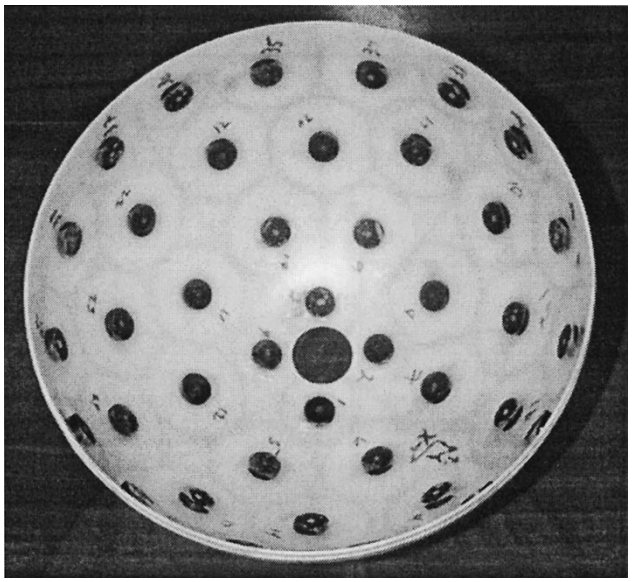

Fig. 8. Inside of the rotor.

A. Construction

A 12-in-diameter plastic sphere is used as the rotor. It is very rigid and splits into two pieces, making it easy to alter the packing of the permanent magnets. The stator structure supports this rotor. An adjustable magnet saddle holds the stator magnets. The saddle has two functions. It positions and orients the stator magnets and provides internal structure for the pedestal. The saddle geometry involves many different angles and intersections that would make it very difficult to machine using classic tools with any accuracy. Inaccuracy in the stator packing would propagate throughout the structure. The saddle was build by first converting CAD drawings of the saddle pieces into G-Code. The pieces were then machined using a wire EDM machine. This assures us very high accuracy on the position of the stator magnets. By making different saddles, the stator packing can be changed. The saddle can slide up and down in the pedestal to adjust the gap between the rotor and stator. The stator electromagnets chosen are 2-in diameter by 1.625-in high and mount to the saddle by a 1/4-20 bolt that passes through the saddle rail and threads into a threaded hole in the magnet. A ring housing machined out of garolite and eight miniature ball castors support the rotor. The ring is press fit into the top of the motor pedestal and positions the castors to be perpendicular to the ball at the contact points. This ring levitates the rotor above the stator magnets and allows the rotor to move relatively friction free. Any inaccuracies in the ring would cause only some of the castors to contact the ball, which would lead to binding. Five removable posts with ball castors at the terminal ends are also used to support the rotor from inside the stator assembly.

Fig. 7 shows the actual stator packing and the castor ring. The rotor was assembled by fixing permanent magnets to the inside of the sphere. Locating points on an actual sphere is a difficult process. We actually drew the Platonic projection on the surface of the sphere, along with the lines required to perform geometric constructions. This enabled us to position the permanent magnets accurately. One-half of the actual rotor packed with magnets is shown in Fig. 8. It is crucial that the magnets be positioned with high accuracy. The ball should have no internal torques. For this to be possible, the principal moments of inertia of the rotor have to be equal $(I_{xx} = I_{yy} = I_{zz})$. Since semiregular packings are used, the rotor, in theory, is balanced, but if the magnets are not positioned accurately, a heavy region will develop, resulting in an internal torque. The gap between the rotor and the faces of the stator magnets is adjusted to be approximately 0.005 in. The final assembly is shown in Fig. 9.

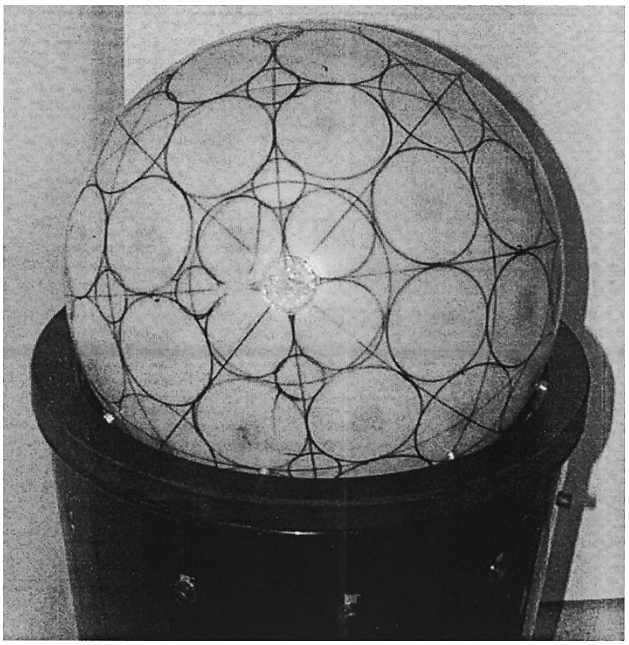

Fig. 9. Assembled motor.

B. Control of the Motor

Printed circuit (PC) relay boards control the states of the stator electromagnets. The boards chosen are Arbor PCI-7250

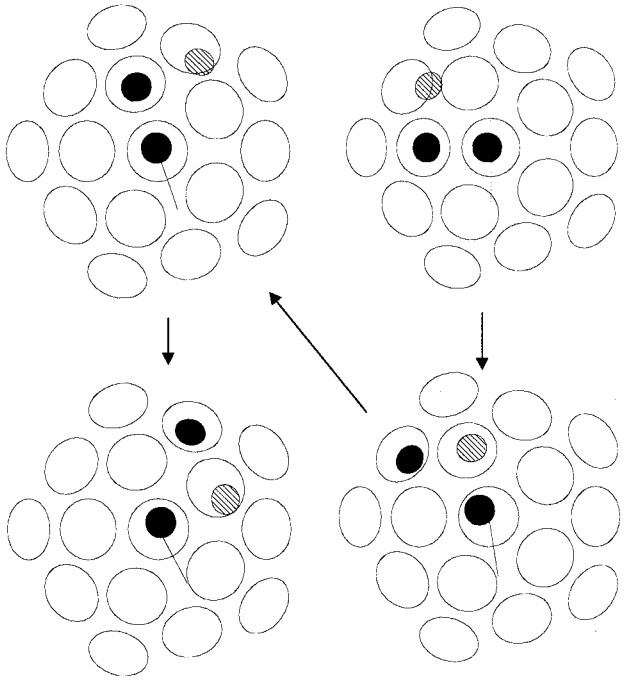

Fig. 10. Example of commutation.

and piggyback boards PCI-7251. Each board contains eight relays. Up to three PCI-7251's can be piggybacked to the PCI-7250, which would allow us to control stator packings up to 32 magnets. A C-language program switches the states of the relays. This enables us to make changes to the motor function and commutation very easily. Power for the electromagnets is supplied by a standard 24-V magnet supply rated up to a 100 W of power.

A computer model of the motor allows us to check the commutation of the motor for different rotor/stator packing and axes of rotation. The algorithm outlined in Section III-A is the computation needed to form the commutation model. The model takes in the packings, rotation axis, rotation direction, allowable errors, and returns the rotor/stator pairs that result in the desired rotor motion. Fig. 10 shows the output of the model for three steps in the motion of the rotor. The motion is along a rotation axis coming out of the page, through the center magnet, with a positive rotation direction. The large ellipses represent the base electromagnets projected onto the plane defined by the rotation axis. The small ellipses correspond to the projection of the rotor magnets that are used in the commutation. The line perpendicular to the rotation axis and projecting to the right in Fig. 10 is a marker that allows us to see the magnitude of the rotation. Filled small ellipses correspond to rotor magnets that are being attracted by the stator at the current instant in time. The hatched small ellipse denotes the next rotor magnet to be attracted by a stator pole to produce rotation along the desired axis. All other magnets are not shown.

V. Conclusions

We have developed a general theory for the kinematic design and commutation of spherical stepper motors where the rotor consists of permanent magnets. This formalism has been applied to the design and commutation of a particular physical prototype. Much work remains in the refinement of this methodology so that motor designs can be generated for specified tasks.

The flexibility built into the design of the motor enable us to perform upgrades relatively easily. We have so far tested one different rotor/stator pair and are planning on testing more. Further testing also needs to be conducted to look at the effect of the size of the rotor magnet relative to the stator. Along with this rotor, magnets of a different composition from those presently being used will be examined.

Acknowledgment

The authors thank Y. Wang for creating the drawings in Fig. 1.

References

[1] B. B. Bederson, R. S. Wallace, and E. L. Schwartz, "A miniature pan-tilt actuator: The spherical pointing motor," *IEEE Trans. Robot. Automat.*, vol. 10, pp. 298–308, June 1994.

[2] B. R. Donald, J. Jennings, and D. Rus, "Information invariants for distributed manipulation," *Int. J. Robot. Res.*, vol. 16, no. 5, pp. 673–702, Oct. 1997.

[3] J. Luntz, W. Messner, and H. Choset, "Parcel manipulation and dynamics with a distributed actuator array: The virtual vehicle," in *Proc. 1997 IEEE Int. Conf. Robotics and Automation*, 1997, pp. 1541–1546.

[4] F. Williams, Laithwaite, and G. F. Eastham, "Development and design of spherical induction motors," *Proc. IEEE*, vol. 47, pp. 471–484, Dec. 1959.

[5] K. Davey , G. Vachtsevanos, and S. Powers, "The analysis of fields and torques in a spherical induction motor," *IEEE Trans. Magn.*, vol. MAG-23, pp. 273–282, Jan. 1987.

[6] Y. Kaneko, I. Yamada, and K. Itao, "A spherical DC servo motor with three degrees-of-freedom," *Trans. ASME Dynam. Syst. Meas. Contr.*, vol. 111, no. 3, pp. 398–402, Sept. 1989.

[7] K.-M. Lee and C.-K. Kwan, "Design concept development of a spherical stepper for robotic applications," *IEEE Trans. Robot. Automat.*, vol. 7, pp. 175–181, Feb. 1991.

[8] R. B. Roth and K.-M. Lee, "Design optimization of a three degrees-of-freedom variable-reluctance spherical wrist motor," *ASME J. Eng. Industry*, vol. 117,pp. 378–388, Aug. 1995.

[9] Z. Zhou and K.-M. Lee, "Real-time motion control of a multi-degree-of-freedom variable reluctance spherical motor," in *Proc. 1996 IEEE Int. Conf. Robotics and Automation*, Minneapolis, MN, Apr. 1996, pp. 2859–2864.

[10] J. Pei, "Methodology of design and analysis of variable-reluctance spherical motors," Ph.D. dissertation, Dep. Mech. Eng., Georgia Inst. Technol., Atlanta, 1990.

[11] S. Toyama, S. Sugitani, G. Zhang, Y. Miyatani, and K. Nakamura, "Multi degree of freedom spherical ultrasonic motor," in *Proc. 1995 IEEE Int. Conf. Robotics and Automation*, Nagoya, Japan, pp. 2935–2940.

[12] S. Toyama, G. Zhang, and O. Miyoshi, "Development of new generation spherical ultrasonic motor," in *Proc. 1996 IEEE Int. Conf. Robotics and Automation*, Minneapolis, MN, Apr. 1996, pp. 2871–2876.

[13] R. L. Hollis, S. E. Salcudean, and A. P. Allan, "A six-degree-of-freedom magnetically levitated variable compliance fine-motion wrist: Design, modeling, control," *IEEE Trans. Robot. Automat.*, vol. 7, pp. 320–332, June 1991.

[14] D. C. Hanselman, *Brushless Permanent-Magnet Motor Design*. New York: McGraw-Hill, 1994.

[15] E. Kreyszig, *Advanced Engineering Mathematics*, 6th ed. New York: Wiley, 1988.

[16] D. L. D. Casper and A. Klug, "Physical principles in the construction of regular viruses," in *Proc. Cold Spring Harbor Symp. Quantitative Biology*, 1962, vol. 27, pp. 1–24.

[17] L. Liljas, "The structure of spherical viruses," *Prog. Biophys. Molec. Biol.*, vol. 48, no. 1, pp. 1–36, 1986.

[18] T. Tarnai, "Spherical circle-packing in nature, practice and theory," *Structural Topology*, no. 9, pp. 39–58, 1984.

[19] B. W. Clare and D. L. Kepert, "The optimal packing of circles on a sphere," *J. Math. Chem.*, vol. 6, no. 4, pp. 325–349, May 1991.
[20] D. A. Kottwitz, "The densest packing of equal circles on a sphere," *Acta Crystallogr. A*, vol. 47, pt. 3, pp. 158–165, May 1991.
[21] L. Fejes-Toth, "Stable packing of circles on the sphere," *Structural Topology*, no. 11, pp. 9–14, 1985.
[22] J. R. Baumgardner and P. O. Frederickson, "Icosahedral discretization of the two-sphere," *SIAM J. Numer. Anal.*, vol. 22, no. 6, pp. 1107–1115, Dec. 1985.
[23] G. S. Chirikjian and S. Zhou, "Metrics on motion and deformation of solid models," *ASME J. Mech. Des.*, vol. 120, no. 2, pp. 252–261, June 1998.
[24] F. C. Park, "Distance metrics on the rigid-body motions with applications to mechanism design," *Trans. ASME, J. Mech. Des.*, vol. 117, pp. 48–54, Mar. 1995.
[25] F. C. Park and B. Ravani, "Bézier curves on Riemannian manifolds and Lie groups with kinematics applications," *Trans. ASME, J. Mech. Des.*, vol. 117, pp. 36–40, Mar. 1995.
[26] J. M. McCarthy, *Introduction to Theoretical Kinematics*. Cambridge, MA: MIT Press, 1990.
[27] K. R. Etzel and J. M. McCarthy, "Spatial motion interpolation in an image space of SO(4)," in *Proc. 1996 ASME Design Engineering Technical Conf. and Computers in Engineering Conf.*, Irvine, CA, Aug. 18–22, 1996.
[28] J. W. Cooley and J. Tukey, "An algorithm for the machine calculation of complex Fourier series," *Math. Comput.*, vol. 19, pp. 297–301, Apr. 1965.
[29] J. R. Driscoll and D. Healy, "Computing Fourier transforms and convolutions on the 2-sphere," *Adv. Appl. Math.*, vol. 15, no. 2, pp. 202–250, June 1994.
[30] D. K. Maslen and D. N. Rockmore, "Generalized FFTs—A survey of some recent results," in *DIMACS Series in Discrete Mathematics and Theoretical Computer Science*, vol. 28. Providence, RI: AMS, 1997, pp. 183–237.
[31] I. M. Gel'fand, R. A. Minlos, and Z. Ya. Shapiro, *Representations of the Rotation and Lorentz Groups and Their Applications*. New York: Macmillan, 1963.
[32] D. A. Varshalovich, A. N. Moskalev, and V. K. Khersonskii, *Quantum Theory of Angular Momentum*. Singapore: World Scientific, 1988.
[33] N. J. Vilenkin and A. U. Klimyk, *Representation of Lie Groups and Special Functions*, vols. 1–3. Dordrecht, The Netherlands, Kluwer, 1991.
[34] G. S. Chirikjian and A. B. Kyatkin, *Engineering Applications of Noncommutative Harmonic Analysis*. Boca Raton, FL: CRC Press, to be published.

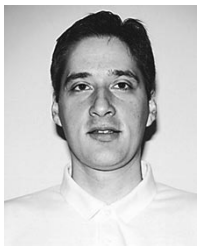

Gregory S. Chirikjian (M'93) was born in New Brunswick, NJ, in 1966. He received the B.S.E. degree in engineering mechanics, the M.S.E. degree in mechanical engineering, and the B.A. degree in mathematics from The Johns Hopkins University, Baltimore, MD, in 1988 and the Ph.D. degree from California Institute of Technology, Pasadena, in 1992.

Since the summer of 1992, he has been with the Department of Mechanical Engineering, The Johns Hopkins University, where he is currently an Associate Professor. His research interests include the kinematic analysis, motion planning, design, and implementation of "hyper-redundant," "metamorphic," and "binary" manipulators. In recent years, he has expanded the scope of his research to include applications of group theory in a variety of engineering disciplines.

Dr. Chirikjian was a 1993 National Science Foundation Young Investigator, a 1994 Presidential Faculty Fellow, and a 1996 recipient of the American Society of Mechanical Engineers Pi Tau Sigma Gold Medal.

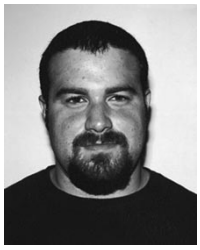

David Stein (S'99) was born in Brooklyn, NY, in 1974. He received B.S.E. degrees in biomedical engineering and in engineering mechanics in 1997 and the M.S.E degree in mechanical engineering in 1999 from The Johns Hopkins University, Baltimore, MD, where he is currently working toward the Ph.D. degree in mechanical engineering.

His research interests are in discrete-state mechanical systems.